ISSN 1027-4510, Journal of Surface Investigation. X-ray, Synchrotron and Neutron Techniques, 2007, Vol. 1, No. 3, pp. 286–293. © Pleiades Publishing, Ltd., 2007.
Original Russian Text © A.E. Galashev, I.A. Izmodenov, O.A. Novruzova, A.N. Novruzov, 2007, published in Poverkhnost'. Rentgenovskie, Sinkhrotronnye i Neitronnye Issledovaniya, No. 5, pp. 74–81.

Computer Study of the Temperature Dependence of Physical Properties of Noncrystalline Silicon Nanoparticles

A. E. Galashev[a], I. A. Izmodenov[b], O. A. Novruzova[b], and A. N. Novruzov[b]

[a] *Institute of Thermal Physics, Ural Division, Russian Academy of Sciences, Yekaterinburg, 620216 Russia; e-mail: galashev@esko.uran.ru*

[b] *Institute of Industrial Ecology, Ural Division, Russian Academy of Sciences, Yekaterinburg, 620219 Russia*

Received June 7, 2006

Abstract—Variations in the structure and kinetic properties of vitreous and amorphous Si_{400} nanoparticles upon heating from 300 to 1700 K are studied by molecular dynamics. The nanoparticle density increases with temperature and approaches the density of bulk solid silicon. A transition from a unimodal to a bimodal distribution of bond lengths is observed upon heating. This transition is more pronounced in the case of the vitreous nanoparticle. The average bond length in the amorphous nanoparticle is, as a rule, larger than that in the vitreous one, and the average number of bonds per atom is lower than that in the vitreous nanoparticle for nearly all studied temperatures. Negative values of the excess potential energy correspond to middle concentric layers of nanoparticles. Liquid layers form in the surface region of nanoparticles in the vicinity of the melting transition. A kinetic test indicating the beginning of nanoparticle melting is formulated.

DOI: 10.1134/S102745100703010X

INTRODUCTION

In recent years, much attention has been given to studying the physical properties of clusters and nanosized particles [1–3]. Of interest is an understanding of the dependence of the properties of nanoparticles on their size. It is especially important to answer the question of how nanoparticles acquiring the properties of the bulk material behave themselves. This area of investigations is developing because of the potential of technological utilization of nanoparticles in optoelectronic devices. The level of experimental, in particular, spectroscopic studies has been raised significantly. The results of some of them have not been understood theoretically so far. For example, the data reported in [4] on the superheating of solid Sn clusters containing 10–30 atoms by ~50 K above the melting temperature of bulk tin arouse great interest.

Processes on the surface of semiconductor crystals are rather complicated and defy theoretical explanation for a number of surfaces. Orbital rehybridization is an important mechanism of reconstruction in covalent semiconductors. An energy gain is, as a rule, accomplished because of a decrease in the number of dangling bonds. By virtue of the curvature and complexity of the surface relief of noncrystalline Si_n nanoparticles, their surface characteristics turn out to be even less predictable. The radial density profile at 1500 K for Si nanoparticles containing 6400 atoms exhibits a certain decrease in density upon moving from the center of the particle to its periphery. The density rapidly drops to zero at a surface layer 0.4 nm thick [5]. Here, the surface tension does not depend on the shape of the tail of the interatomic interaction potential. Bulk atoms of Si_n nanoparticles do not exert such a collective effect (attraction), which is commonly observed in metal nanoparticles. Potentials taking into account three-body interactions reasonably describe surface properties of semiconductors.

Computer simulation methods (in particular, molecular dynamics (MD)) are the main ones in theoretical studies of physical properties of nanoparticles. Actually, computer simulation of nanoparticles containing up to several thousands of atoms and using empirical potentials has become at present an important instrument for subsequent theoretical constructions [6, 7]. More rigorous computer simulation based on ab initio interactions can be performed for clusters containing to several tens of atoms. This method is frequently used in modeling small clusters of semiconductor materials [8]. A study of structural and kinetic properties of a Si_{480} nanoparticle was performed by molecular dynamics in the temperature range $600 < T < 2000$ K using the Stillinger–Weber potential [9]. The authors of this work believe that the structure of the nanoparticle core is similar to the structure of the bulk silicon glass and the self-diffusion coefficient of atoms in the nanoparticle at high temperatures is comparable with the corresponding characteristic of liquid silicon. Studying properties of larger formations of silicon atoms is important both from the point of view of nanoelectronics and for the development of a procedure for obtaining nonsintering spherical nanoparticles by chemical vapor deposition.

The goal of this work is to investigate the stability of noncrystalline silicon nanoparticles heated from 300 to 1700 K, to determine the variation of their main physicochemical properties caused by heating, and to study the effect of the preparation method of nanoparticles on their temperature stability.

COMPUTER MODEL

The Stillinger–Weber potential used for the description of Si–Si interactions can be represented in the form of a sum of two functions $\Phi_{(2)}$ and $\Phi_{(3)}$ describing the two- and three-body interactions [10]

$$\begin{aligned}\Phi_{(2)}(r_{ij}) &= \varepsilon f_{(2)}(r_{ij}/\sigma),\\ \Phi_{(3)}(\mathbf{r}_i, \mathbf{r}_j, \mathbf{r}_k) &= \varepsilon f_{(3)}(\mathbf{r}_i/\sigma, \mathbf{r}_j/\sigma, \mathbf{r}_k/\sigma),\end{aligned} \quad (1)$$

where ε is chosen so that function $f_{(2)} = -1$ at $r_{ij} = \sigma$ and σ obeys the condition $f_{(2)}(2^{1/6}) = 0$. Function $f_{(2)}$ is a function of a scalar, and function $f_{(3)}$ possesses the full translational and rotational symmetry. The pair part of the potential is represented in the form

$$f_{(2)}(r) = \begin{cases} A(Br^{-p} - r^{-q})e^{\frac{1}{r-a}}, & r < a \\ 0, & r \geq a \end{cases}, \quad (2)$$

where A, B, and p are positive constants. The three-body interatomic interaction function is given as

$$\begin{aligned}f_{(3)}(\mathbf{r}_i, \mathbf{r}_j, \mathbf{r}_k) &= h(\mathbf{r}_{ij}, \mathbf{r}_{ik}, \Theta_{jik})\\ &+ h(\mathbf{r}_{ji}, \mathbf{r}_{jk}, \Theta_{ijk}) + h(\mathbf{r}_{ki}, \mathbf{r}_{kj}, \Theta_{ikj}),\end{aligned} \quad (3)$$

where Θ_{ijk} designates the angle between vectors $\mathbf{r}_i$ and $\mathbf{r}_k$ converging at vertex j. Function h is determined as

$$h(\mathbf{r}_{ij}, \mathbf{r}_{ik}, \Theta_{jik}) = \begin{cases} \lambda e^{\frac{\gamma}{r_{ij}-a} + \frac{\gamma}{r_{ik}-a}}\left(\cos\Theta_{jik} + \frac{1}{3}\right), & r_{ij}, r_{ik} < a \\ 0, & r \geq a. \end{cases} \quad (4)$$

It is parameter Θ that provides information on the existence of bond distortion. Function $f_{(3)} = 0$ when $\cos\Theta$ is a perfect tetrahedral angle $\cos\Theta = -1/3$. The Stillinger–Weber potential describes the complex of deformations more accurately than can be done with potentials based only on two-atom interactions. The characteristics of the Stillinger–Weber potential are given in Fig. 1 in the form of function $\Phi_{(2)}(r)$ representing the pair contribution of interatomic interactions and dependence $\Theta_{ijk}(r)$, $r = r_{ij} = r_{kj}$ for five values of three-body contributions: 8.67, 4.33, 2.17, 0.43, and 0.04 eV/at. The curves shown in Fig. 1 are calculated for silicon clusters containing from two to six atoms.

The numerical integration of the equations of motion was performed using the Verlet algorithm [11], in which the velocities of particles are directly calculated. On the one hand, this scheme is one of the most stable, and, on the other hand, it allows the temperature in the model to be controlled rather accurately. The time step Δt was 10^{-16} s.

COMPUTATIONAL PROCEDURE

Silicon nanoparticles containing 400 atoms were the subject of simulation. Two types of Si_{400} nanoparticles with noncrystalline packing of atoms were preliminarily obtained in computer experiment [12]. The first type was represented by a vitreous nanoparticle obtained by rapidly cooling a liquid silicon particle from 3000 to 300 K. An amorphous silicon nanoparticle belonged to the second type. Its initial configuration was specified by a random-number generator, after which structural relaxation was performed at $T = 300$ K. Real calculations were started at a temperature of 300 K. After each 10^6 time steps, the temperature of nanoparticles was increased by 100 K using the corresponding scaling of atomic velocities in the interval $2 \times 10^4\ \Delta t$.

Physicochemical characteristics of nanoparticles were calculated in time intervals $10^6\ \Delta t$ defined as periods of structural relaxation. The average Si–Si bond length $\langle L_b \rangle$ and the average number of bonds $\langle n_b \rangle$ per atom were determined by constructing Voronoi polyhedra (VP) after each thousand time steps.

Among the nearest neighbors revealed through VP, the neighbors whose distance did not exceed 0.3 nm were selected. This value is close to the value of the Morse potential parameter [13] describing the Si–Si interactions. In this way, the bonds L_b and their number n_b were determined. To a detailed investigation of physical properties of nanoparticles, their volume was approximated by a sphere divided into concentric layers of equal thickness d. A sphere whose radius was four times larger than d was considered as the first layer. The centers of the spheres and the concentric layers coincided with the center of masses of the nanoparticle. The number of atoms in each spherical layer was determined after each $10\ \Delta t$. The potential energy and the coefficients of mobility of atoms in each layer were calculated after the same time intervals. The average number of atoms in the first layer of a vitreous nanoparticle was 19 and that for the amorphous particle was 11. The difference between the average numbers of atoms in other layers was no more than 40. The excess potential energy, which is defined as

$$\Delta U/\langle U \rangle = (U_n - \langle U \rangle)/\langle U \rangle, \quad (5)$$

gives a clearer picture of the state of the layers. Here, U_n is the potential energy of atoms constituting the nth layer, and $\langle U \rangle$ is the average potential energy of the nanoparticle. The numbering of layers starts from the center of the nanoparticle.

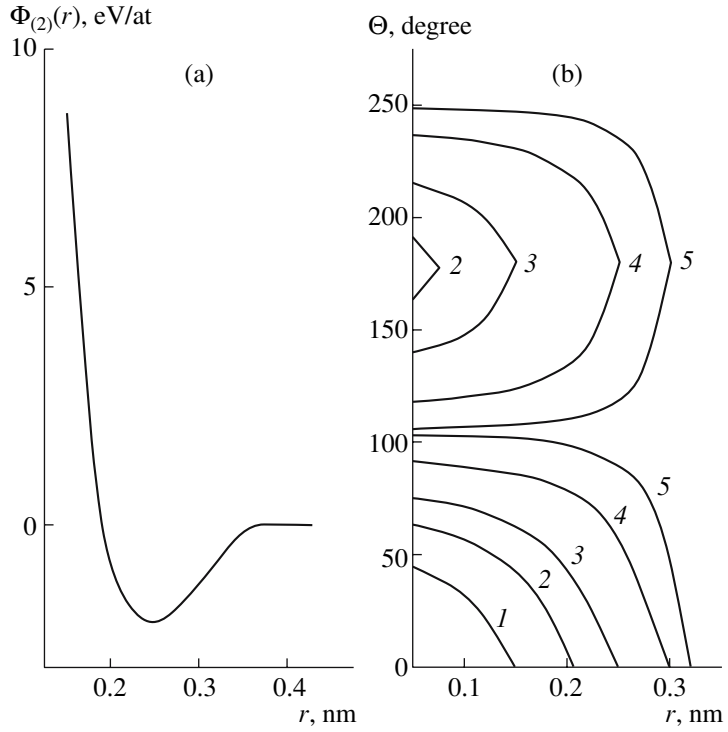

Fig. 1. Characteristics of the Stillinger–Weber potential for silicon: (a) the $\Phi_{(2)}(r)$ function representing a pair contribution to the interaction; (b) dependence of the angle Θ with the vertex at the center of atom j on the distance $r = r_{ij} = r_{kj}$ to the centers of atoms i and k forming this angle; the contribution of three-body interactions is shown by isolines: *1*, 8.67; *2*, 4.33; *3*, 2.17; *4*, 0.43; and *5*, 0.04 eV/at.

The overall coefficient of mobility was calculated through the average square of atom displacements according to the equation [14]

$$D = \lim_{t\to\infty}\frac{1}{6t}\frac{1}{N}\sum_{i=1}^{N}[\mathbf{r}_i(t+t_0)-\mathbf{r}_i(t_0)]^2, \qquad (6)$$

where $\mathbf{r}_i(t)$ is the radius vector of the ith particle at the time instant t. The displacements of atoms in a spherical cluster can be presented as two components [14]: the radial component $\langle(\Delta\mathbf{r})^2\rangle_r$, which characterizes displacements of atoms in the direction to (or from) the center of the cluster, and the tangential component $\langle(\Delta\mathbf{r})^2\rangle_t$ which describes displacements in the directions perpendicular to the radial one. Therefore,

$$D_r = \frac{1}{3}\lim_{t\to\infty}\frac{\langle\mathbf{r}^2(t)+\mathbf{r}^2(0)-2\mathbf{r}(t)\mathbf{r}(0)\rangle}{t}, \qquad (7)$$

$$D_t = \frac{1}{3}\lim_{t\to\infty}\frac{\langle\mathbf{r}(t)\mathbf{r}(0)[2-2\mathbf{u}(t)\mathbf{u}(\mathbf{0})]\rangle}{t}. \qquad (8)$$

Here, $\mathbf{u} = \mathbf{r}(t)/|\mathbf{r}(t)|$ is a unit vector. Coefficients D, D_r, and D_t characterize the mobility of atoms in nanoparticles. We calculated the radial distributions of these quantities averaged over the concentric layers of the spherical cluster. Because $\langle(\Delta\mathbf{r})^2\rangle = \langle(\Delta\mathbf{r})^2\rangle_r + \langle(\Delta\mathbf{r})^2\rangle_t$, the coefficients of mobility are related by the equation $D = D_r + D_t$.

STUDY OF TEMPERATURE VARIATIONS IN NANOPARTICLES

Structure. One of the most conspicuous changes of the state of nanoparticles upon heating is the growth of the density of nanoformations. The increase in the density of a Si_{400} nanoparticle in both the vitreous and amorphous states with increasing temperature from 300 to 1700 K was 23.7% (Fig. 2). The density of a vitreous Si_{400} nanoparticle at $T > 1500$ K falls in the range of densities of crystalline (3) and liquid (4) silicon. At a temperature of 1700 K, vitreous Si nanoparticles have a dense core and a loose outer layer covering a greater part of the nanoparticle (Fig. 3). An amorphous nanoparticle has a larger volume than a vitreous particle of the corresponding size. In this case, atoms are distributed more uniformly over the volume of the nanoparticle. However, here, the density in the periphery is also lower than in the core. At a low temperature ($T = 500$ K), the maximum of the distribution of Si–Si bond lengths lies at 0.228 nm for a vitreous Si_{400} nanoparticle and at 0.235 nm for the corresponding amorphous nanoparticle (Fig. 4). With increasing temperature, the main

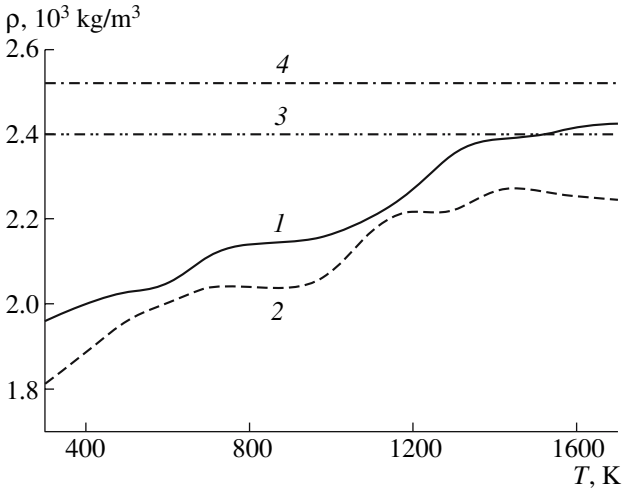

Fig. 2. Temperature dependence of the density of Si_{400} nanoparticles: *1*, vitreous nanoparticle; *2*, amorphous nanoparticle; *3*, density of crystalline silicon at $T = 300$ K; and *4*, density of liquid silicon in the vicinity of T_m.

maximum of the distribution of bond lengths shifts toward lower values of L_b. Additional maxima also appear on the right-hand side of the main peak. Thus, the main maximum of the distribution of L_b at $T = 1000$ and 1500 K is localized at 0.222 nm in a vitreous nanoparticle and at 0.228 nm in an amorphous nanoparticle. The temperature dependence of the average Si–Si bond length in nanoparticles exhibits an oscillating behavior (Fig. 5a). As the temperature grows from 300 to 1700 K, the value of $\langle L_b \rangle$ increases by 0.08% in the case of a vitreous Si_{400} particle and by 0.58% for the corresponding amorphous nanoparticle. The average bond length in an amorphous silicon nanoparticle is higher than $(L_b)_{\text{cryst}}$ in the corresponding bulk crystal [15] in the entire temperature range, and $\langle L_b \rangle > (L_b)_{\text{cryst}}$ in a vitreous nanoparticle at $T > 550$ K. With increasing temperature, there is a tendency to an increase in the average number of Si–Si bonds per atom in nanoparticles (Fig. 5b). As the temperature increased from 300 to 1700 K, the value of $\langle n_b \rangle$ increased by 17% for a vitreous Si_{400} nanoparticle and by 14% for an analogous amorphous particle. Note that the number of bonds per atom in a vitreous Si nanoparticle exceeds the value of $\langle n_b \rangle$ for an amorphous nanoparticle in a virtually entire range of studied temperatures. However, the value of $\langle n_b \rangle$ for both types of nanoparticles is lower than the corresponding characteristic of a silicon macrocrystal. This fact predetermines the higher stability of vitrified nanoparticles at high temperatures.

The occurrence of tetrahedral packing in nanoparticles can be judged by the presence of a second peak at $r = 0.36$ nm in their radial distribution function. Actually, the two first coordination spheres of a irregular tetrahedral packing are almost identical to the coordination spheres of the diamond lattice [16]. A rotation of the tetrahedra changes distances to the third neighbors,

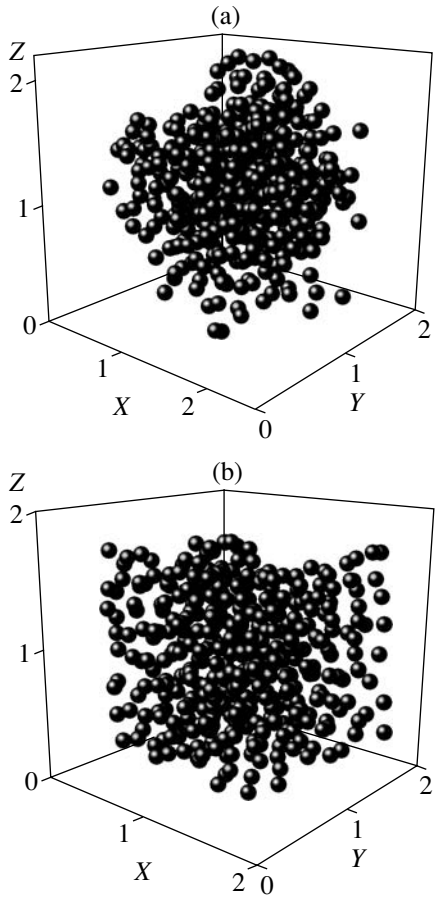

Fig. 3. Configurations of Si_{400} nanoparticles obtained by structural relaxation at $T = 1700$ K: (a) glass; (b) amorphous silicon. The coordinates of Si atoms are given in nanometers.

so that the third peak in the curve of the radial scattering function (RSF) disappears when going from crystalline to amorphous silicon. At low temperatures ($T \le 500$ K), the second peak of the RSF is present in the $g(r)$ function of a vitreous nanoparticle and is absent in the RSF of an amorphous nanoparticle. At $T = 1000$ K, the second peak of $g(r)$ is absent for both of these particles, and, at $T = 1500$ K, a peak at $r = 0.36$ nm appears for both nanoparticles but it is more pronounced for a vitreous nanoparticle. Apparently, the low-temperature tetrahedral structure that occurs in a vitreous nanoparticle is not stable and decays because of large strains in the region of 1000 K. However, with a further increase in temperature, a different tetrahedral packing appears in both vitreous and amorphous nanoparticles.

The angular distribution of the nearest geometrical neighbors is the finest indicator reacting to a change in the structure. Angles θ are considered whose vertex lies at the center of a VP that are formed by pairs of neighbors forming faces of the VP. The angular distribution for both types of nanoparticles substantially changes its shape when the temperature increases from 300 to

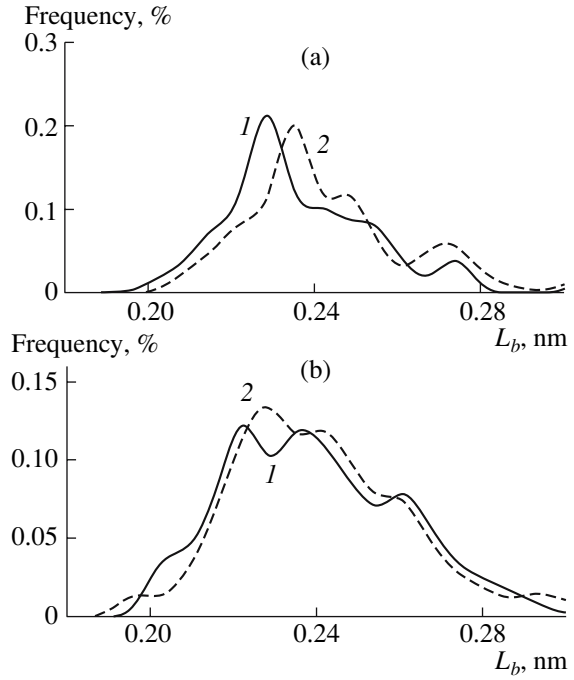

Fig. 4. Distribution of Si–Si bond lengths in (*1*) vitreous and (*2*) amorphous Si_{400} nanoparticles corresponding to temperatures of (a) 500 K and (b) 1500 K.

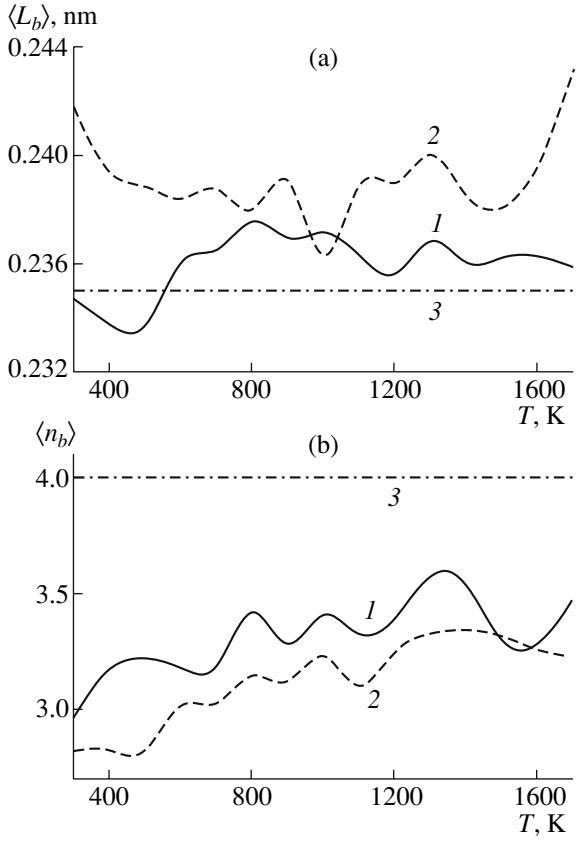

Fig. 5. Temperature dependences of (a) the average Si–Si bond length and (b) the average number of bonds per atom for a Si_{400} nanoparticle in different states: *1*, vitreous; *2*, amorphous; and *3*, silicon macrocrystal.

1700 K (Fig. 6). The most significant changes of the θ distribution that occur with increasing temperature are as follows: an increase in the intensity of the first peak located in the vicinity of 60°; the growth of the second peak located in the region of 114°; and the initiation of the third peak in the vicinity of θ = 153°. All these changes are observed for both vitreous and amorphous nanoparticles. The shape of the θ distribution obtained at high temperatures is characteristic of the majority of irregular packings, including that for the rigid sphere model [17]. The position of the first maximum of the θ distribution for the rigid sphere model coincides with the localization of the corresponding maximum of the θ spectrum of a nanoparticle of vitrified silicon at 1700 K. However, the second maximum of the angular distribution for the rigid sphere model is localized at 123° rather than 114°. The angular distribution of the coordinates of the third atom with respect to the axis connecting a pair of its neighbors determined by means of constructing VP (θ distribution) for an amorphous nanoparticle and for a vitreous particle in a wide temperature range has the main peak at 60°. In the case of a dense random packing, this peak corresponds to the tangency of the fixed pair with a third atom, while the peak at 123° can be interpreted as the place of preferable localization of the next nearest geometrical neighbors forming a six-membered ring. For vitreous and amorphous silicon nanoparticles, the first peak of the θ spectrum at 60° mainly reflects the arrangement of the second-order neighbors, while the second peak at 114° more likely corresponds to the arrangement of the first-order neighbors, whose number $3 < \langle n_b \rangle < 4$.

The distribution of VP over the number of faces (*f* distribution) and the distribution of faces over the number of sides (*m* distribution) obtained with an exclusion of small VP edges with the length $l < \dot{l}/2$ ($\dot{l}$ is the average length of the VP edge) confirm the noncrystalline character of atomic packings in nanoparticles. All atoms in the diamond lattice are combined into rings by six atoms. The fraction of six-membered rings determined by the *m* distribution of the simplified VP is 29–31% for a vitreous nanoparticle and 27–30% for an amorphous nanoparticle. An amorphous nanoparticle at $T = 1000$ K contains the least number of such rings, and a vitreous particle at $T = 1700$ K contains the largest number of such rings. The predominance of five-membered rings is observed, for example, in the structure of a simple liquid. Upon heating from 300 to 1700 K, the number of five-membered rings increased from 39 to 56% for a vitreous nanoparticle and from 47 to 56% for an amorphous nanoparticle. In both cases, the fraction of five-membered rings at $T = 1000$ K exceeded 50%. The presence of one or another type of rings affects the entire structure of nanoformations. All the *m* distribu-

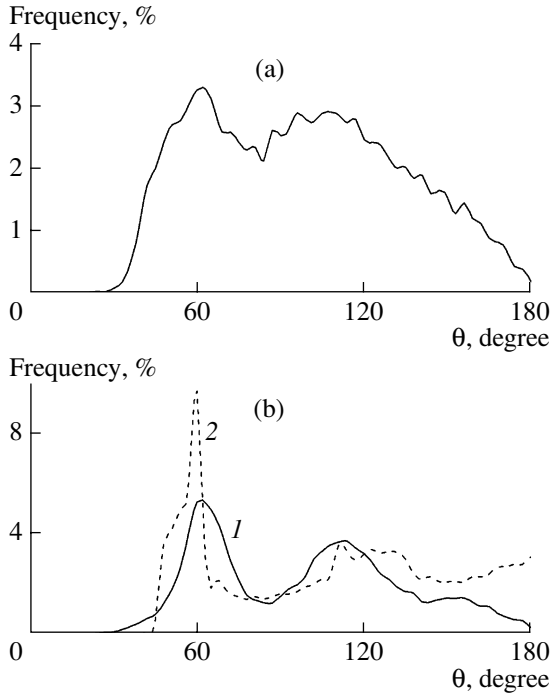

Fig. 6. Angular distribution of the nearest geometrical neighbors in a vitreous Si_{400} nanoparticle: (a) T = 300 K; (b) *1*, MD calculation, T = 1700 K; *2*, extended irregular packing in the rigid sphere model [17].

tions of a Si_{400} nanoparticle have a maximum at $m = 5$, and the majority of f distributions, at $f = 12$. Only the f spectrum of an amorphous Si_{400} nanoparticle at T = 1700 K is characterized by a maximum at $f = 13$, which reflects the liquid state of the nanoparticle. In a perfect static closely packed lattice, each VP has 12 faces. Thermal disorder gives rise to new faces, and, as a result, the f distribution broadens.

Energy and kinetic properties. An increase in the kinetic energy of nanoparticles results in a redistribution of the potential energy in their concentric layers (Fig. 7). At T = 300 K, the excess potential energy of nanoparticles (both vitreous and amorphous) has a profile gradually passing from negative (in the inner part) to positive (on the outside) values. Already at a temperature of 1000 K, five inner layers have positive values of ΔU, the number of outer layers with $\Delta U > 0$ drops to five, and four middle layers turn out to be most favorable in energy ($\Delta U < 0$). At T = 1700 K, the middle region of the nanoparticle with $\Delta U < 0$ extends to five layers, and the most favorable seventh layer has a potential energy that is lower than $\langle U \rangle$ by more than 100%. The most significant difference in the distribution of a vitreous nanoparticle is revealed at T = 1000 K. In this case, the sixth layer, for which a neighboring layer has a positive value of U, has itself the lowest value of energy ΔU.

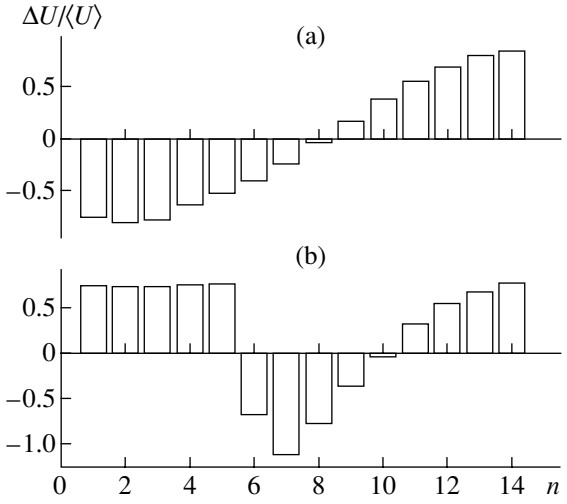

Fig. 7. Relative excess potential energy of concentric layers for an amorphous Si_{400} nanoparticle at different temperatures: (a) 300 K; (b) 1700 K.

The kinetic stability of nanoparticles is traced by the behavior of coefficients D, D_r, and D_t as functions of temperature. The melting temperature T_m of crystalline silicon is 1688 K. The Stillinger–Weber potential gives a close value of T_m (~1665 K) [9]. Model silicon nanoparticles of ~3–4 nm in size melt in the vicinity of 1660 K [9]. At relatively low temperatures ($T \le 500$ K), the tangential component of the coefficient of mobility dominates the radial component in virtually all the concentric layers of a vitreous Si nanoparticle. In the case of an amorphous nanoparticle, the D_r and D_t components have comparable values already at T = 500 K. In the vicinity of 1000 K, the tangential component of D in concentric layers of both a vitreous nanoparticle and an amorphous nanoparticle becomes already more pronounced than D_r. It should be noted that the values of D_r and D_t in the surface region of these nanoparticles appear to be higher than those for other layers. At a temperature of 1700 K, the tangential component D_t dominates the radial one in the eight outer layers of a vitreous nanoparticle (Fig. 8). Moreover, the value of D_t in the four outer layers is almost twice as high as the corresponding values for the middle layers, which is indicative of the presence of a liquid layer on the surface of a vitreous nanoparticle. The same tendency is also revealed for an amorphous nanoparticle at T = 1700 K; however, there are intrinsic peculiarities in this case. In the five outer layers, the value of D_t is higher than D_r. However, the distribution of the values of D_t in the outer layers is different here, while the value of D_t in the third layer exceeds the values of D_t in all other layers. Liquidlike motion is observed in almost all (except for some middle) layers of an amorphous nanoparticle. Thus, at a temperature of 1700 K, an amorphous particle occurs in a liquid state, while the process of melting still proceeds in a vitreous nanoparticle.

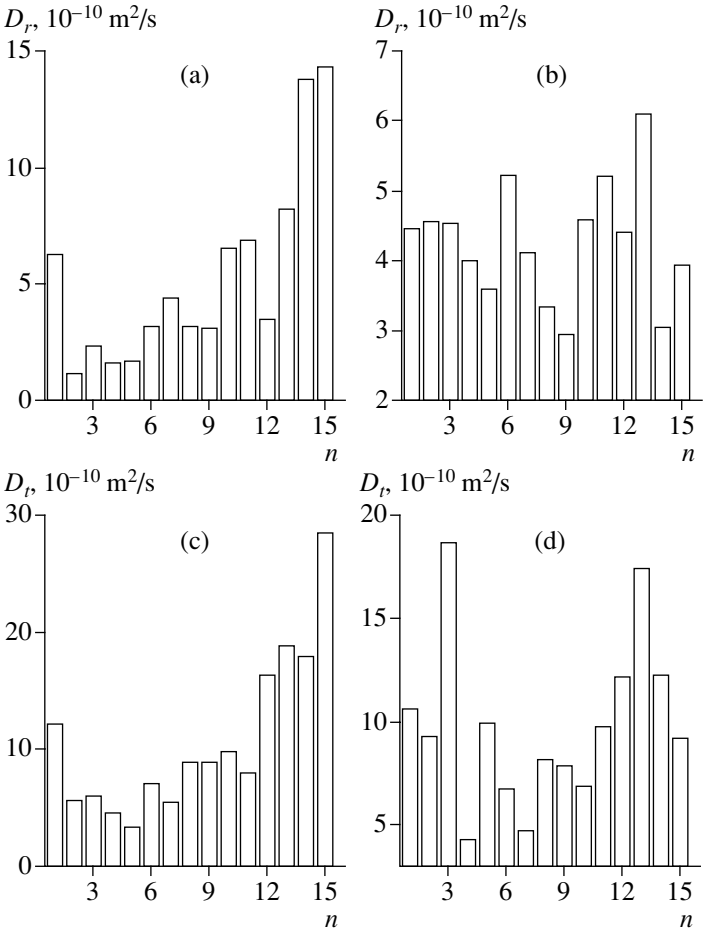

Fig. 8. (a, b) Radial and (c, d) tangential components of the coefficient of mobility D of atoms in concentric layers for (a, c) vitreous and (b, d) amorphous Si_{400} nanoparticles at $T = 1700$ K.

CONCLUSIONS

The results obtained in this work demonstrated that the physicochemical properties of silicon nanoparticles subjected to a thermal treatment depend on the preparation method of these particles. Therefore, depending on the area of application, a particular technology should be selected for obtaining nanomaterials. Nanoparticles of Si glass can be used under high-temperature conditions as thermally more stable formations. The density of nanoparticles increases with increasing temperature. A break in the dependence $U(T)$ for the noncrystalline silicon nanoparticles studied in this work indicates that their temperature interval of melting is 1600–1700 K.

An increase in the intensity of the first peak in the RSF by more than 10% with respect to the height of this peak at room temperature can serve as an empirical test of the stability of amorphous and vitreous silicon nanoparticles with respect to the formation of a liquid phase. However, the kinetic test of stability according to which a nanoparticle acquires a liquidlike behavior when an increase in temperature results in a sharp enhancement of radial motion of atoms in one or several outer layers of the nanoparticle is a more accurate indicator of the onset of melting. A detailed analysis of distributions of the radial component of the coefficient of mobility of atoms over concentric layers shows that the kinetic instability predetermining melting comes at a temperature of 1400 K for an amorphous silicon nanoparticle and at 1500 K for a vitreous Si nanoparticle. At the next stage, melting spreads from three to four outermost layers of the nanoparticle. The displacements of atoms in the radial and especially tangential directions become substantially enhanced in these layers. Subsequently, the inner layers of the nanoparticle start to melt.

ACKNOWLEDGMENTS

This work was supported by the Presidium of the Ural Division of the Russian Academy of Sciences within the framework of an integration project run in the Ural and Far-East Divisions of the Russian Academy of Sciences.

REFERENCES

1. L. J. Lewis, P. Jensen, and J.-L. Barrat, Phys. Rev. B **56**, 2248 (1997).

2. G. Meloni, M. J. Ferguson, S. M. Sheehan, and D. M. Neumark, Chem. Phys. Lett. **399**, 389 (2004).
3. L. Mitas, C. Grossman, I. Stich, and J. Tobik, Phys. Rev. Lett. **84**, 1479 (2000).
4. A. A. Shvartsburg and M. F. Jarrold, Phys. Rev. Lett. **85**, 2530 (2000).
5. T. Hawa and M. R. Zachariah, J. Chem. Phys. **121**, 9043 (2004).
6. Y. Kawazoe, T. Kondow, and K. Ohno, *Clusters and Nanomaterials: Theory and Experiment* (Springer, Berlin, 2002).
7. A. E. Galashev, Poverkhnost. Rentgen. Sinkhrotr. Neitron. Issled. **1**, 77 (2005).
8. E. Kaxiras and K. Jackson, Phys. Rev. Lett. **71**, 727 (1993).
9. M. R. Zachariah and M. J. Carrier, J. Phys. Chem. **100**, 14856 (1996).
10. F. H. Stillinger and T. A. Weber, Phys. Rev. B **31**, 5262 (1985).
11. L. Verlet, Phys. Rev. **159**, 98 (1967).
12. A. E. Galashev, V. A. Polukhin, I. A. Izmodenov, and O. A. Galasheva, Poverkhnost. Rentgen. Sinkhrot. Neitron. Issled. **1**, 41 (2006).
13. J. D. Kubicki and A. C. Lasaga, Am. Mineral. **73**, 941 (1988).
14. C. L. Briant and J. J. Burton, Nature Phys. Sci. **243**, 100 (1973).
15. E. F. Sheka and E. A. Nikitina, Dokl. Akad. Nauk **378**, 208 (2001).
16. J. Ziman, *Models of Disorder* (Mir, Moscow, 1982; Cambridge Univ. Press, Cambridge, 1979).
17. J. Bernal and S. King, *Physics of Simple Liquids: Statistical Theory* (Mir, Moscow, 1971), p. 116 [in Russian].